Journal of GeoEngineering, Vol. 18, No. 2, pp. 071-082, June 2023
http://dx.doi.org/10.6310/jog.202306_18(2).3

VERTICAL DYNAMIC IMPEDANCE FOR VIBRATIONS ISOLATION OF FOUNDATIONS USING IN-FILLED TRENCHES

Benslama Boualam [1], Bourahla Nouredine [2], Messioud Salah [3*], Dias Daniel [4]

ABSTRACT

This paper proposes an improved vibration-barrier technique to reduce the vibrations of shallow foundations. For this purpose, three-dimensional finite element with absorbing boundaries were used to model and perform dynamic analyses of the whole system comprising the soil, the in-filled trenches (barrier) and the foundation. The barriers are commonly set up to protect a target structure, whereas the present study focuses on reducing the vibrations of the foundation itself. This achieved by disposing the barriers around the entire vibration source (foundation). The performance of the proposed technique evaluated under a generated vertical unit steady-state force applied on a massless square foundation. The dynamic compliance function's real and imaginary coefficients compared to those found in the literature and plotted separately. The obtained results using two different geotechnical conditions confirmed that surrounding the foundation by a barrier is more effective to reduce the foundation-vibration.

Key words: Foundation, isolation barrier, harmonic vibration, dynamic impedance.

1. INTRODUCTION

Vibrating machines, traffic, blasting, construction activities and earthquakes are the origin of ground vibrations. An excessive vibration can disturb high-precision instruments and annoy people working in the immediate area, as well as provoking damages to adjacent structures (Terzi 2020). Consequently, the main objective of machine-foundation design is to limit these vibrations (Gazetas 1975).

The mitigation of vibration effects on structures achieved by different methods such as moving the source of vibration away from the structure, improving the damping features of soils or isolating the exposed structure. The isolation of structure can be accomplished using a base-isolation system, an interrupting wave barrier, or shaping the landscape surrounding the structure. The optimal solution depends on the geology and geography of the site; the excitation characteristics, in particular, the frequency; and the available space around the structure (Klein *et al.* 1997).

In fact, there are various types of interrupting wave barriers, such as periodical networks (Bougressi *et al.* 2017; Amrane *et al.* 2019), sheet piles, tubular piles, row of piles, and open or in-filled trenches with different materials like concrete, gravel, expandable aggregate, plastic foam (McNeill *et al.* 1965; Jazebi *et al.* 2022), soil bentonite mixture, and flexible rubber chips (Alzawiand El-Naggar 2011). The in-filled barrier is more practical and useful due to some difficulties in maintaining an open trench caused by the soil instability or water table height, even though the open trench barrier is the most effective (Saikia 2014). Concrete is an example of stiff materials and it has a positive performance in large frequency ranges (Jazebi *et al.* 2022). In the present study, an in-filled barrier with concrete is used as an isolation system and also to increase the soil stiffness.

Soil structure interaction (SSI) is a critical issue considered in the evaluation of the dynamic response of structures whenever the effect of building-foundations interface thought to be significant. Consequently, several numerical methods, such as the boundary element method (BEM), the thin layer method (TLM) and the finite element method (FEM) have been developed and used for this purpose. During the long history of the wave propagation problems, the FEM was used by several researchers (Barkan 1962; Klein *et al.* 1997; Adamand Estorff 2005; Alzawi and El-Naggar 2011; Saikia 2014; Terzi 2020). Modeling the unbounded soil field appropriately is a challenge for civil engineers. In soil-mechanics problems, the assumption of a homogeneous half-space frequently made for the sake of simplicity (Woods 1968; Lin *et al.* 2013).

Many researchers have considered the problem of vibration barriers from different perspective. Terzi (2020) used a two-dimensional (2D) finite element modeling Fig. 1(a) to investigate the dynamic behavior of the strip footing in presence of a vibration barrier. The results showed that the impedance functions for the cases of an open trench and homogeneous half-space agreed. However, some discrepancies noticed between the case of concrete in-filled trenches and homogeneous half-space. (Dudchenko *et al.* 2021, 2022) used a three-dimensional (3D) realistic finite element modeling to explore the performance of horizontal and vertical barriers in preventing the propagation of surface waves energy into a protected zone. The conclusion was that the efficiency in attenuating the response of a point on the protected zone depends mainly on a better balance between the geometry and the material properties of the barrier with the soil conditions. (Jazebi *et al.* 2022) studied the effect of Rayleigh wavelength on the performance of open and in-filled trenches with impact loading. The study revealed that the depth of the vertical barrier depends significantly on the Rayleigh wavelength and preferably installed at a normalized distance greater than 1.0 to achieve high efficiency.

Manuscript received December 5, 2022; revised April 11, 2023; accepted April 12, 2023.
[1] Ph.D. Student, Department of Civil Engineering, Ecole Nationale Polytechnique (ENP), Algiers, Algeria.
[2] Professor, Department of Civil Engineering, Ecole Nationale Polytechnique (ENP), Algiers, Algeria.
[3*] Lecturer, LGCE Laboratory (corresponding author), University of Jijel BP98 18000, Algeria (e-mail: smessioud@yahoo.fr).
[4] Professor, 3SR Laboratory, Polytech Grenoble Alpes University, France.

This study aims to investigatethe effectiveness of isolating foundation's vibrations using in-filled trenches.To achieve this, three-dimensional finite element numerical models with absorbing boundaries are proposed to analyze the dynamic behavior of foundation vibrations isolation using in-filled trenches. The foundation installed on the soil surface and subjected to a vertical dynamic loading. The formulation is based on the substructuring method (Messioud *et al.* 2016), and it takes into account the viscoelastic behaviour of the system.

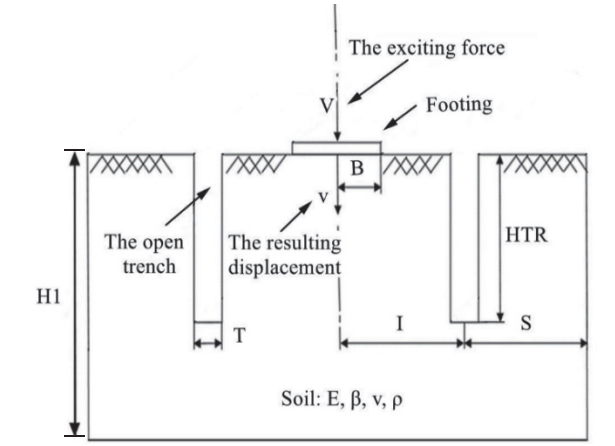

(a) Two-dimensional view

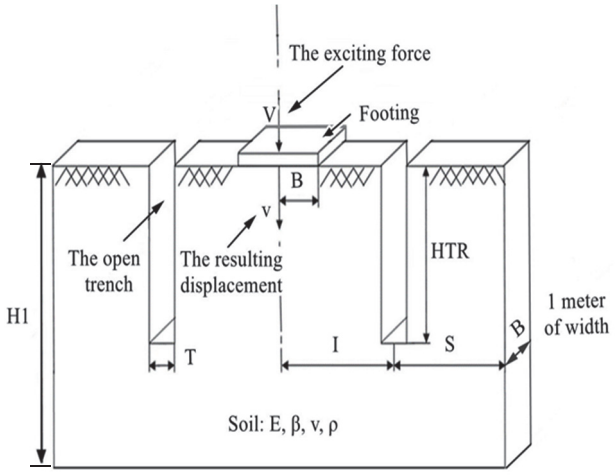

(b) Three-dimensional view for 1 m

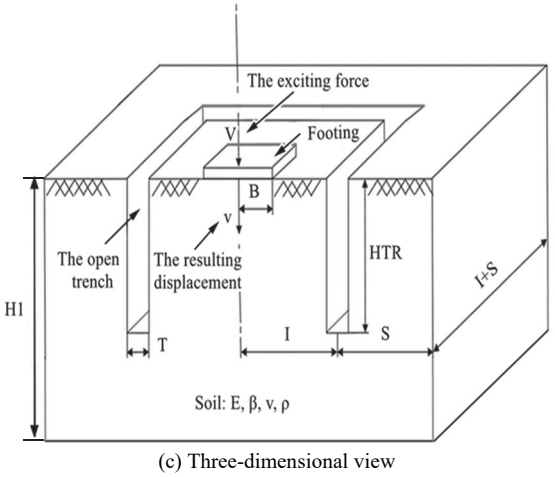

(c) Three-dimensional view

Fig. 1 (a) 2D modeling used in Terzi 2020, (b) extended 3D modeling with 1 meter of width, the case *I*/*B* = 10 (half of the model), (c) Vibration isolation using a trench encircling the vibrating source, the case *I*/*B* = 10 (half of the model)

More focus placed on protecting the targeted structure rather than reducing the footing's vibration itself. The novelty of the present study is to evaluate the performance of the technique proposed in Fig. 1(c) for two objectives. The first objective is to protect the targeted structures set up behind the barrier, and the second objective is to evaluate the attenuation of the vibration-wave amplitudes by confinement effect. This study based on extending the 2D model shown in Fig. 1(a) to construct the 3D model depicted in Fig. 1(b), and then surrounding the entire footing with the barrier as shown in Fig. 1(c). The obtained results presented in terms of dynamic compliances and validated against reference results.

2. DESCRIPTION OF THE PROBLEM AND THE USED METHOD

Since the compliance function coefficients of the model shown in Fig. 1(c), a linear, viscoelastic, frequency-dependent analysis is addressed in the article written by Fukuwa and Nakai (1989).

The subject of the problem is a rigid massless square footing that is completely bonded to the free surface of a homogeneous, isotropic viscoelastic linear half-space (E, β, v, ρ). The completely bonded type of contact between the footing and the half-space is essential as it ensures a perfect continuity of the displacements and stresses between rigid footing and half space without detachment, gapping or slippage (Fukuwaand Nakai 1989; Luco 1974).

The footing is harmonically excited by V applied on its base (gravity center), and v is the displacement produced (Elsabee 1975). Then, v/V the compliance function deduced. The response v of the model depends mainly on the excitation frequency, the geometry of the footing and the soil properties (Gazetas 1975). The positive direction of the external forces and the displacements are shown in Fig. 1(c). The model geometric characteristics are in the list of symbols below.

3. DESCRIPTION OF THE MODEL

3.1 Mechanical and Geometrical Characteristics

The calculation of compliance function coefficients is presented in Fig. 2(b) for a homogeneous half-space (Model 2) and Fig. 2(c) for soil over a rigid bed-rock (Model3), with different locations of the barrier: I/B = 4, 10, and 20. The normalized distances (I/B) primarily selected based on the concept of a closer or farther barrier distance from the footing. The compliance functions of the model presented in Fig. 2(a) generated and then validated against results published in the literature by (Terzi 2020). Subsequently, the compliance functions of the model presented in Fig. 2(b) produced and compared to those of the model depicted in Fig. 2(a). The findings of this study will assist civil engineers in designing structural foundations, particularly for machine-foundations, by providing insights into how to reduce the impact of foundation vibrations.

FEM is a very useful numerical method used for modeling very complicated geometries and reading the output-data is very easily available at any positions. It is robust, powerful, especially, for low frequencies (Terzi 2020). The present study aims to use the afore mentioned study's model, but, in three dimensions, the one presented in Figs. 2(a) and 2(b), with shear (V_{SV}) and Rayleigh waves only.

The 3D finite element models shown in Fig. 2 used to illustrate the main idea of this study. The gray elements represent the soil, the green elements represent the barrier, the red elements represent the footing and blue elements represent the bedrock.

The characteristics of the foundation, the soil and the in-fill materials taken from (Terzi 2020) are given in the Table 1.

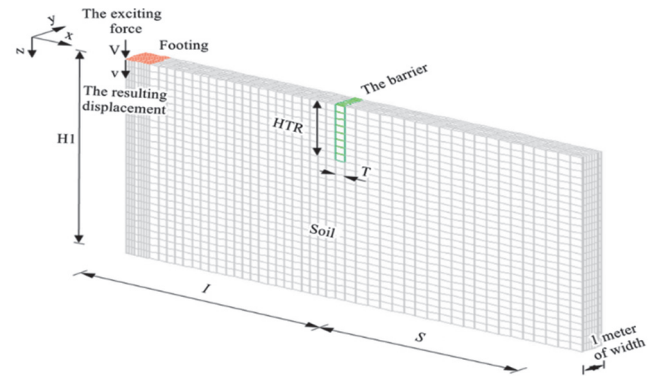

(a) Model 1

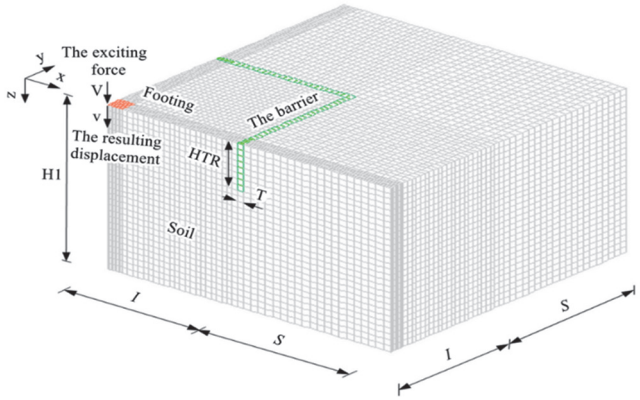

(b) Model 2

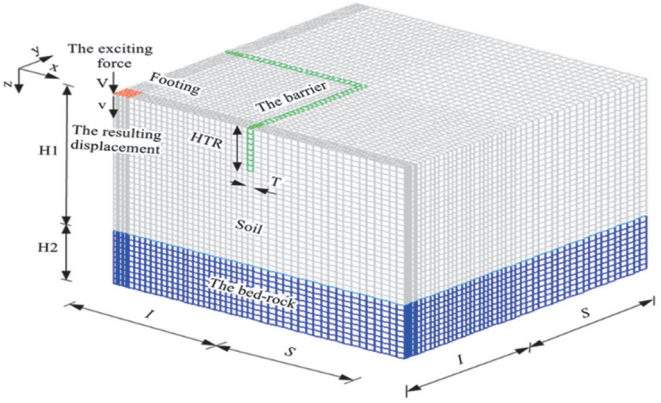

(c) Model 3

Fig. 2 Numerical models for the case *I*/*B* = 10 (quarter of the model)

Table 1 Mechanical characteristics

Material	*E* (MPa)	*v*	ρ (kg/m^3)	β
Soil	46	0.25	1,800	0.05
Bed-rock	100	0.2	2,200	0
Rigid footing	Infinity	0.25	0	0
Concretebarrier	46E+2	0.25	2,700	0.05

Table 2 Geometrical characteristics

Material	Length (m)	Width (m)	Depth (m)	Thickness (m)	Side (m)
Soil	10	10	$H_1 = 13B$	not concerned	not concerned
Bedrock	10	10	$H_2 = 5B$	not concerned	not concerned
Rigid footing	not concerned	not concerned	not concerned	0.2	$2B = 2$
Concretebarrier	not concerned	not concerned	$HTR = 1.33\ \lambda_{min}$	$T = 0.133\ \lambda_{min}$	not concerned

In fact, the depth and thickness of the barrier are functions of the shortest wave wavelength (λ_{min}) which propagate into the soil. The depth should be at least 30% of λ_{min}, in order to receive at least 50% of the input energy reduction (McNeill *et al.* 1965). In the present study: λ_{min} = 3 m; *HTR* should be superior to 30% of λ_{min}; based on the idea of making a relationship between *B* and *HTR*; ($HTR = 4B = 1.33\ \lambda_{min} \geq 0.3\ \lambda_{min}$) is just selected; $T = HTR/10 = 0.133\ \lambda_{min}$ as the barrier's width does not have a significant impact on source-vibration amplitude reduction (Woods 1968).

The selection of the model and the size of the finite elements are in agreement with the wavelength to minimize the distortion wave's effect (Messioud *et al.* 2017, 2019). The applied maximum frequency depends on the maximum size of the element (Kuhlemeyer and Lysmer 1973) which shows that the size mesh element must be less than one tenth of the wavelength λ,

$$f = \frac{V_s}{10 \cdot \Delta l} = \frac{\omega}{2\pi} \tag{1}$$

The impedance ratio, *IR*, introduced in this study to examine whether or not the barrier material is harder than the surrounding soil. *IR* frequently used in geotechnical engineering (Adamand Estorff 2005) and defined as

$$IR = \rho_b V_b / \rho_s V_s \tag{2}$$

In the following case study, *IR* is 12.25.

3.2 Finite Element Mesh

Since the model includes an isolated square massless foundation, a symmetric 3D finite element model is adopted for a more realistic representation (Wolf and Deek 2004).

The selection of the appropriate dimensions of the finite element is based on achieving a good balance between minimizing the memory space required and reducing the computational time, capturing the shortest wavelength propagated through the soil more accurately (Mino *et al.* 2009), and ensuring linear displacement within the finite element. The size of the mesh elements should be small enough to allow for the transmission of waves in an appropriate manner and without distortion of these waves. This achieved by applying 3 to 4 discretizations for the half-length of the shortest wave (Pecker 1984). Therefore, a 3D linear elastic, 8-nodes cubic finite-element is used (CUB8). The FE modeling is carried out using CAST3M software (version 2017) which is a calculation and geometric-modeling code for the analyzing structures using the finite element method. The dynamic calculation is performed using Code-Aster software (version 13.4).

For vertical isolated foundation vibration, almost 93% of the energy is carried away in the free field by surface and shear waves (V_R, V_{SH}, V_{SV}), and only 7% is transported by P-waves (Dobry and Gazetas 1986). Rayleigh waves are the primary concern in foundations isolation problems (Woods 1968). In this study, only vertical shear waves (V_{SV}) and Rayleigh waves (V_R) are analyzed. Therefore, pressure waves are not included. The energy density of body waves dissipates quickly into the soil due to a greater value of the geometric damping in 3D modeling compared to 2D modeling (McNeill *et al.* 1965).

When dealing with soil-structure-interaction (SSI), one of the most important issues is the reflection of waves. This occurs when waves bounce back into the model due to the absence of absorbent boundaries and the borders of the FE model not being far enough from the source of the vibration, even when using large model dimensions. Achieving perfect wave absorption is practically impossible (Castellani1974). Therefore, imposing artificial absorbing boundaries at all the model-borders is essential. This was proposed by (Messioud *et al.* 2017, 2019; Neghmouche *et al.* 2022). Consequently, the present study uses the finite element method with absorbing boundaries.

In fact, choosing the suitable location of the artificial absorbing boundaries strongly depends on the characteristics of the wave incident on the artificial boundaries; the frequency-range of the excitation and the damping of the soil material (Wolf 1989). In practice, wave motion problems are always three-dimensional, if low dimensional artificial absorbing boundaries are used for a multi-dimensional model, then, the results will be highly inaccurate, therefore, using 3D boundary, such as 3D_ABSO (in Code - Aster), is required (Jingbo *et al.* 2006).

The model of the artificial absorbing boundaries assigned to the FE model, being studied here, is named 3D_ABSO (Code-Aster). It corresponds to finite elements whose mesh supports are surfaces (each surface of the CUB8 element is a linear-elastic 4-nodes quadratic element (QUAD4)). Only small linearized deformations are supported in the frequency domain. In the present study, the deformation order is less than 10^{-2} meter. This is an acceptable order compared to the footing size. This result ensures the validity of these absorbing boundaries (3D_ABSO); and the linear analysis required for treating the impedance functions problem.

4. VALIDATION OF THE NUMERICAL MODEL

The validation of the numerical Model1, shown Fig. 2(a) was conducted by calculating the foundation compliance function coefficients for various scenarios: without trench, with an open trench, and with the barrier, for a ratio I/B = 4. For I/B values of 10 and 20 only the case with a barrier was considered. The obtained results compared with those presented by (Terzi 2020) for the 2D model in Fig. 1(a), as they are independent of the third dimension (y) under plane strain conditions.

In order to minimize the memory storage, the mesh used is refined only in the excited zone where the exterior force is applied. Then, it is gradually enlarged in x and y directions along footing-trench distances.

If $f_{\max}$ is the highest wave frequency travelling through the soil and V (V_{SV} or V_{SH} or V_R in the present study) is its propagation velocity, the dimension of the finite element used for the modeling, should satisfy the condition of Eq. (1). Considering the condition mentioned above and using an 8-nodes finite-element, the mesh assigned to the model is:

- $B/8 \times B/8 \times B/2$, for the finite-elements beneath the footing.
- $B/2.5 \times B/2.5 \times B/2$, for the finite-elements between the footing and the trench, the trench is included.
- $B/2 \times B/2 \times B/2$, for the finite-elements between the trench and the boundaries (far from the excited zone).

After examining the finite element dimensions provided above, the aspect ratio of the elements ranges from 0.8 to 4, which falls within the acceptable range of aspect ratios according to FEM rules. It is well-known that the impedance functions matrix $K_{ij}(\omega)$ is defined as follows (Gazetas 1983):

$$K_{ij}(\omega) = K_{stij}(\omega)\left(k_{ij}(\omega) + i\, a_0\, c_{ij}(\omega)\right)(1 + i2\,\beta) \tag{3}$$

where i and j = v or h vibrations, for the present study, a_0 ranges from 0.1 to 2.5 (Terzi 2020).

$$K_{stvv} = \frac{4GB}{1-\nu}\left(1+1.28\frac{B}{H}\right)\left(1+0.47\frac{E_f}{B}\right)\left[1+\left(0.85-0.28\frac{E_f}{B}\right)\frac{E_f/H}{1-E_f/H}\right] \tag{4}$$

$$K_{sthh} = \frac{8GB}{2-\nu}\left(1+\frac{1}{2}\frac{B}{H}\right)\left(1+\frac{2}{3}\frac{E_f}{B}\right)\left(1+\frac{5}{4}\frac{E_f}{H}\right) \tag{5}$$

where K_{stvv} and K_{sthh} are the vertical and horizontal static-stiffness corresponding to a unit vertical and horizontal displacement respectively, E_f is the embedment of the footing and G is the shear modulus of elasticity (Kausel and Ushijima 1979). Additionally, $K_{ij}(\omega)$ can be written in the following formula as:

$$K_{ij}(\omega) = \mathrm{Re}\left(K_{ij}(\omega)\right) + i\,\mathrm{Im}\left(K_{ij}(\omega)\right) \tag{6}$$

where $\mathrm{Re}(K_{ij}(\omega))$ and $i\ \mathrm{Im}(K_{ij}(\omega))$ are the real and imaginary parts of $K_{ij}(\omega)$ respectively. They are functions of the excitation frequency (ω), the characteristics of the soil-foundation contact; and the characteristics of the soil profile (Dobry and Gazetas 1986).

$F_{ij}(\omega) = K_{ij}^{-1}(\omega)$ is the compliance functions matrix of the model, $F_{ij}(\omega)$, also, can be written in the previous form:

$$F_{ij}(\omega) = \mathrm{Re}\left(F_{ij}(\omega)\right) + i\,\mathrm{Im}\left(F_{ij}(\omega)\right) \tag{7}$$

In order to normalize $F_{ij}(\omega)$, the factor πG^* is used, where G^* is the complex shear modulus of elasticity.

$$G^* = G\,(1 + i\,2\beta), \qquad G = \frac{E}{2(1+\nu)} \tag{8}$$

So,

$$F_{ij}(\omega)\pi G^* = \left[\mathrm{Re}\left(F_{ij}(\omega)\right) + i\,\mathrm{Im}\left(F_{ij}(\omega)\right)\right]\pi G(1+i2\beta) \tag{9}$$

After some simplification, the Eq. (9) becomes:

$$\mathrm{Re}\left(F_{ij}(\omega)\pi G^*\right) = \mathrm{Re}\left(F_{ij}(\omega)\right)\pi G - \mathrm{Im}(F_{ij}(\omega))\pi G 2\beta \tag{10a}$$

$$\mathrm{Im}\left(F_{ij}(\omega)\pi G^*\right) = \mathrm{Re}\left(F_{ij}(\omega)\right)\pi G 2\beta - \mathrm{Im}\left(F_{ij}(\omega)\right)\pi G \tag{10b}$$

Figure 3 shows the real and imaginary coefficients of the dynamic compliance function for the vertical vibrations in Model 1: without trench, with a trench, and with a concrete barrier.

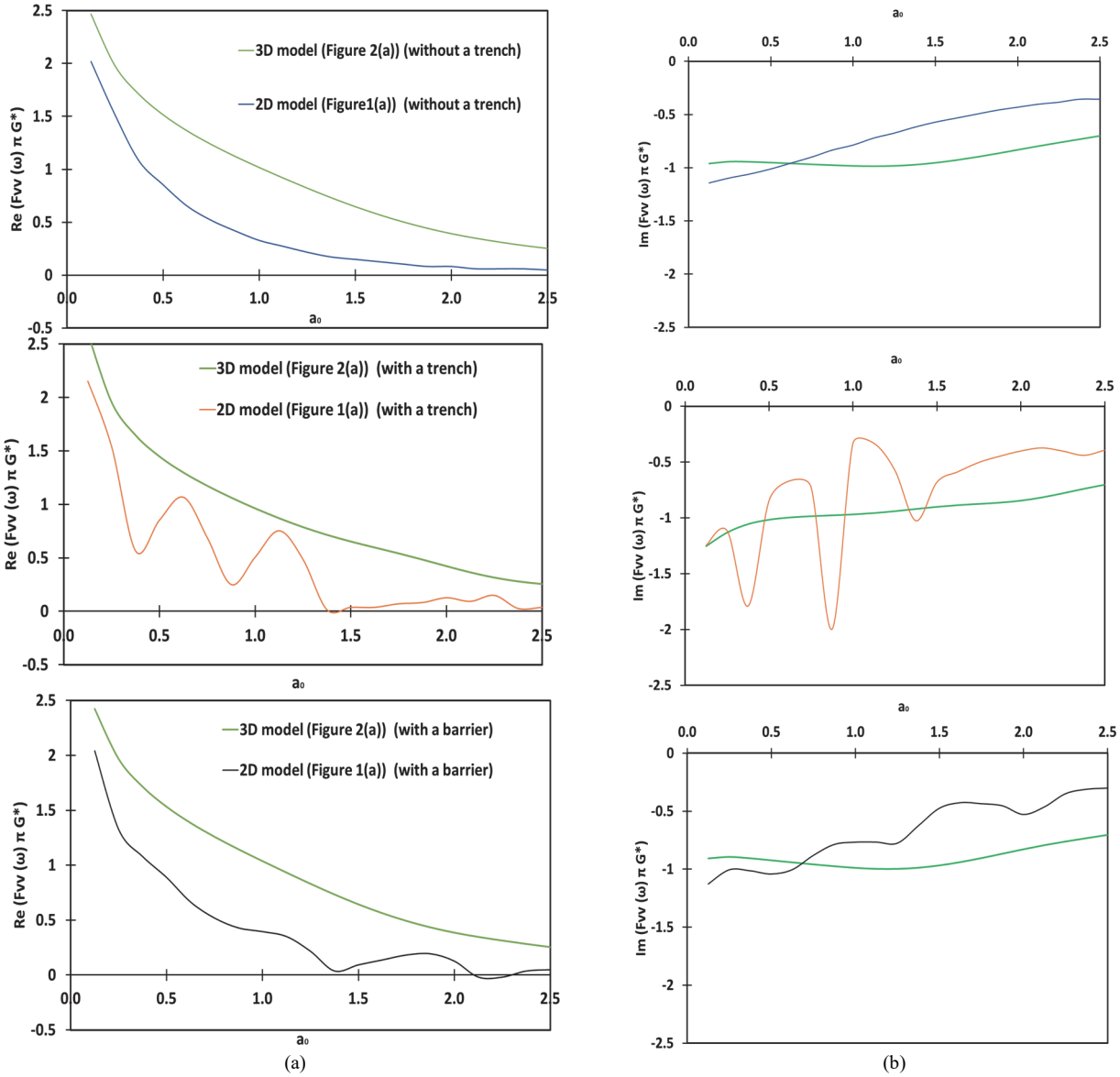

Fig. 3 (a) Real and (b) imaginary coefficients of the vertical compliance function for the cases from top to bottom: without trench; with an open trench; and with a barrier (model 1), $I/B = 4$

The imaginary part of Fig. 4 highlights that the barrier being close to the footing at $I/B = 4$, makes Model 1 less flexible, especially for low frequencies $a_0 < 0.875$. Stability and smoothness of the results depicted in Figs. 5 and 6, clearly point out the reliability of model 1, with the cases $I/B = 10$ and 20, to be used then to construct model 2 mainly analyzed in the present investigation.

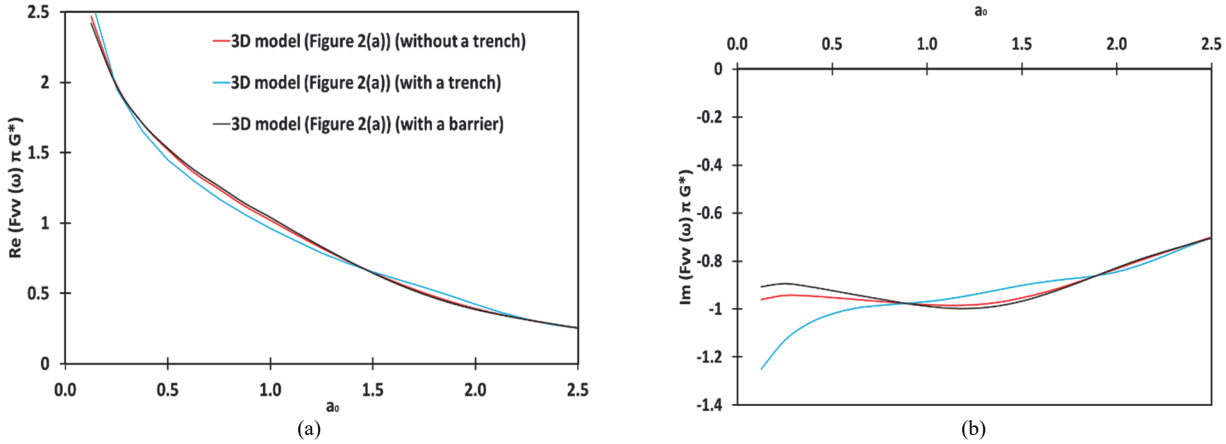

Fig. 4 (a) Real and (b) imaginary compliance functions for the cases: without trench, with trench and with a barrier (Model 1), $I/B = 4$

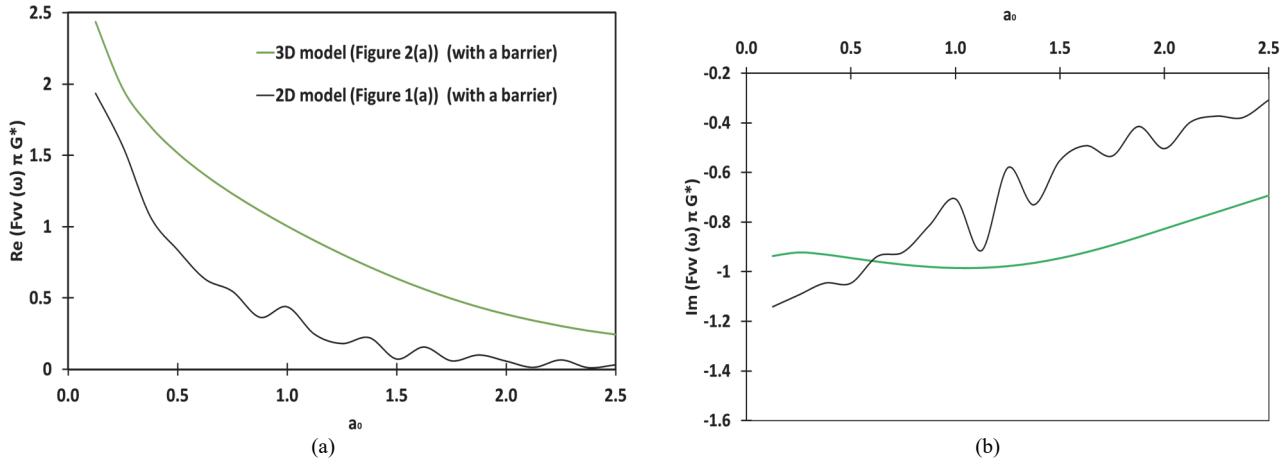

Fig. 5 (a) Real and (b) imaginary coefficients of the vertical compliance function for the case with a barrier (Model 1), *I*/*B* = 10

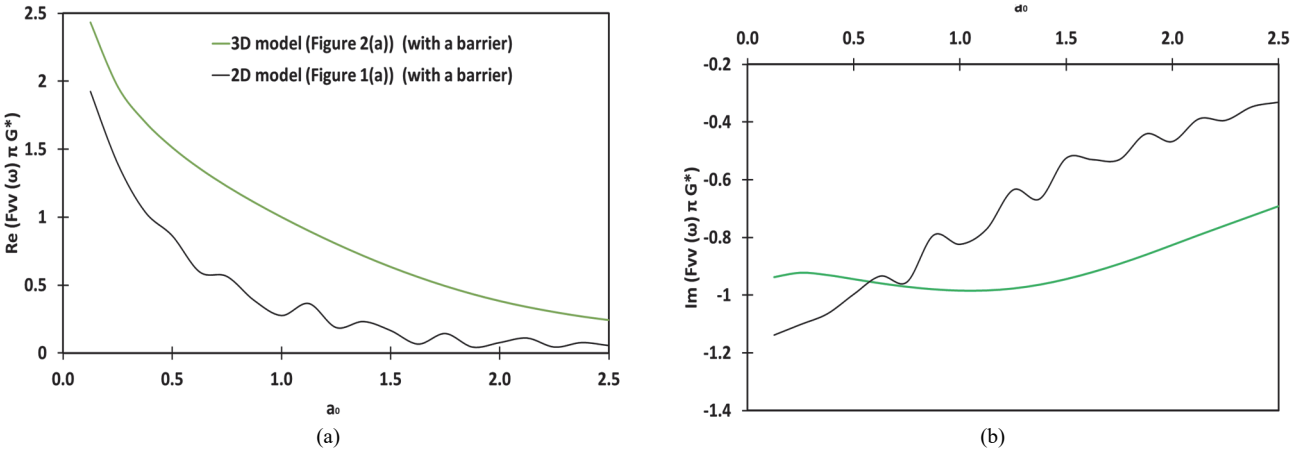

Fig. 6 (a) Real and (b) imaginary coefficients of the vertical compliance function for the case with a barrier (Model 1), *I*/*B* = 20

Figure 7 indicates that changing the barrier location from a distance of $I/B = 4$ to $I/B = 10$ or 20 does not result in any changes in the compliance function coefficients. This explains no effectiveness of using a barrier in the form presented in Model 1. A clear and smooth variation of the compliance function coefficients of Model 2 shown in Fig. 2(a) is noticeable across the range of a_0. This is particularly evident in the case with a trench, as shown in Fig. 3, and it is due to the continuity of the soil in the y direction, which makes Model 2 in Fig. 2(a) less flexible than the 2D model shown in Fig. 1(a) used in (Terzi 2020).

The smoothness and stability of the results for the compliance function coefficients are very noticeable in Figs. 3 to 7. It is better to use 3D models presented in Fig. 1(b) instead of the 2D shown in Fig. 1(a). The results also confirm the reliability of the numerical Model 1 as demonstrated in Fig. 2(a) and the accuracy of the compliance function coefficients used to compare with those producedby Model 2 in Fig. 2(b).

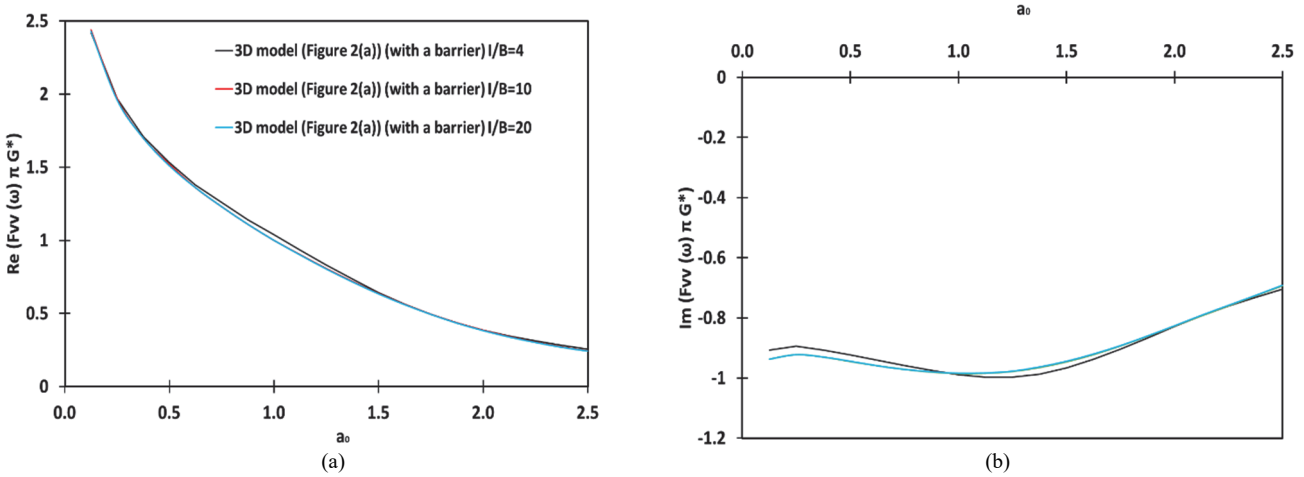

Fig. 7 (a) Real and (b) imaginary compliance functions for the cases: with a barrier for *I*/*B* = 4, 10, and 20 (Model 1)

5. PARAMETRIC STUDY

To investigate which location of the barrier is most effective in reducing the source-vibrations, three different values of the parameter I/B were selected; 4, 10, and 20, corresponding to the barrier being source-isolation to receiver-isolation. The compliance functions of Model 2 presented in Fig. 2(b) are compared with those of Model1 given in Fig. 2(a).

The fluctuation of the compliance function curves corresponding to the case with a trench in Fig. 8 is due to the empty volume of the open trench. The propagating waves toward x and y directions Model (2) do not find a material to pass through, but find free edges instead.

The imaginary part corresponding to the concrete barrier case of Fig. 8 shows finite values of the compliance function coefficients corresponding to the first and the second natural-frequencies. This is due to the zero geometric damping adopted for low frequencies for a homogeneous half-space.

Figure 9 indicates that the use of encircling barrier isolation is effective when comparing the real and imaginary compliance functions of the cases without a trench versus with a barrier. The gap between these two curves (black and red) is quite small as $E_b = 100\ E_s$.

Figures 10 and 11 (imaginary compliance functions) explains less vibration levels in the direction y of waves propagation in Model 2 compared with Model 1 due to the barrier surrounding all the footing, in particular for $a_0 < 1$ (the green curves).

Figure 12 shows that for a homogeneous half-space model, using an encircling barrier at a distance of I/B = 10 or 20 is more effective in terms of vibration reduction level than using it at a distance of $I/B = 4$ particularly for $a_0 < 1$, since less vibration waves are reflected toward the footing (red and blue curves). f_n is the natural frequency of the model and defined by Gazetas (1975):

$$f_n = \frac{(2n-1)\,V_R}{4H} \tag{11}$$

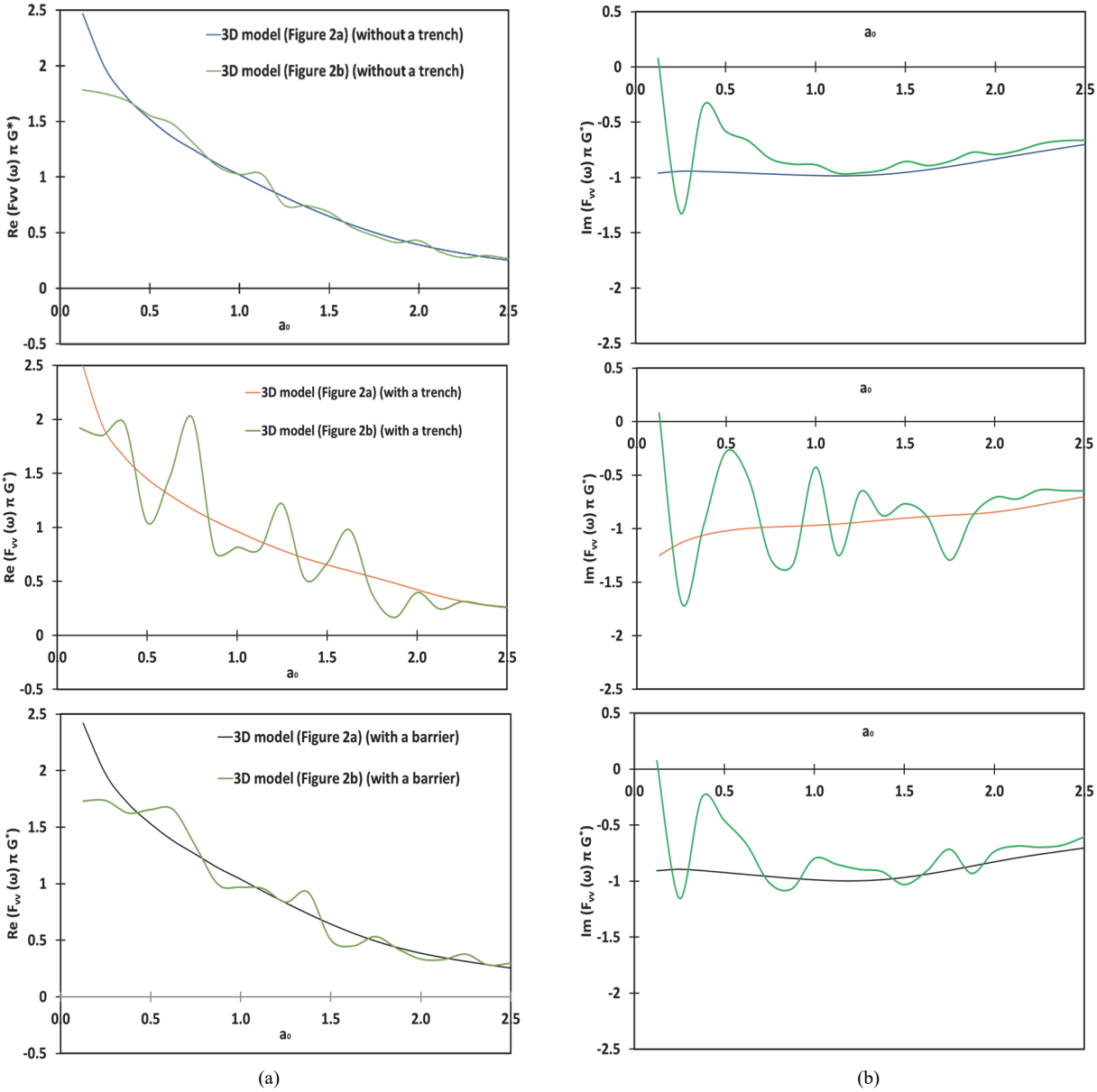

Fig. 8 (a) Real and (b) imaginary coefficients of the vertical compliance functions for the cases from top to bottom: without trench, with an open trench, with a barrier; I/B = 4 (Comparison between Model 1 and Model 2 in Fig. 2(a) and 2(b))

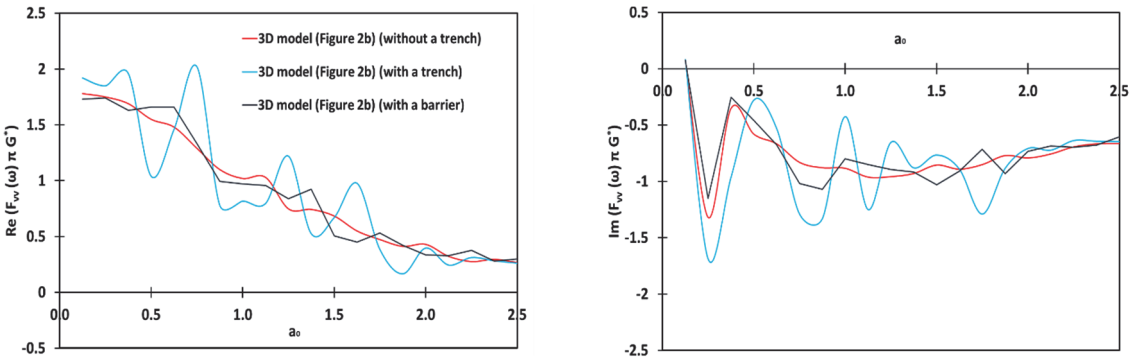

(a) (b)

Fig. 9 (a) Real and (b) imaginary compliance functions for the cases: without a trench, with a trench and with a concrete barrier (Model 2), $I/B = 4$

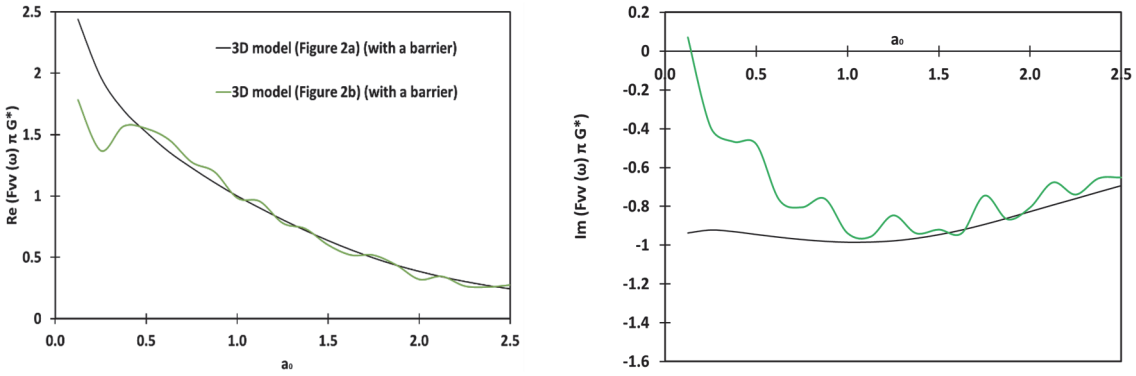

(a) (b)

Fig. 10 (a) Real and (b) imaginary coefficients of the vertical compliance function for the case with a concrete barrier, $I/B = 10$ (Comparison between Model 1 (Fig. 2(a)) and Model 2 (Fig. 2(b)))

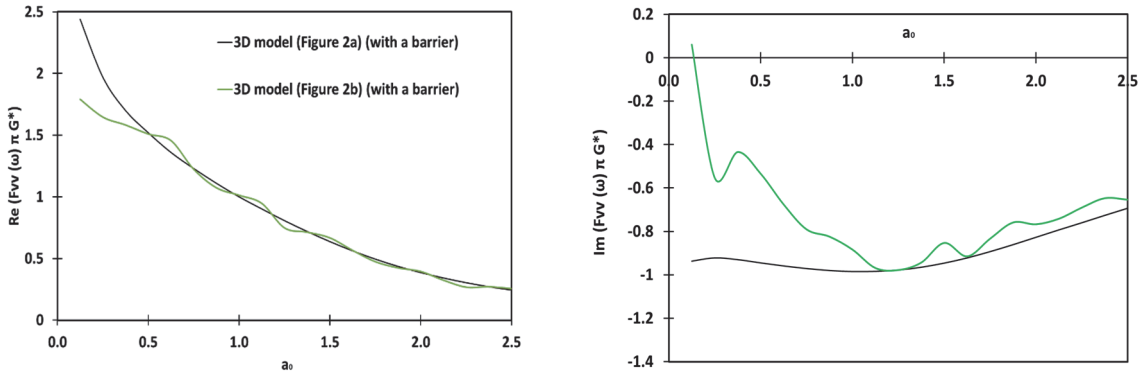

(a) (b)

Fig. 11 (a) Real and (b) imaginary coefficients of the vertical compliance function for the case with a concrete barrier, $I/B = 20$ (Comparison between Model 1 (Fig. 2(a)) and Model 2 (Fig. 2(b))

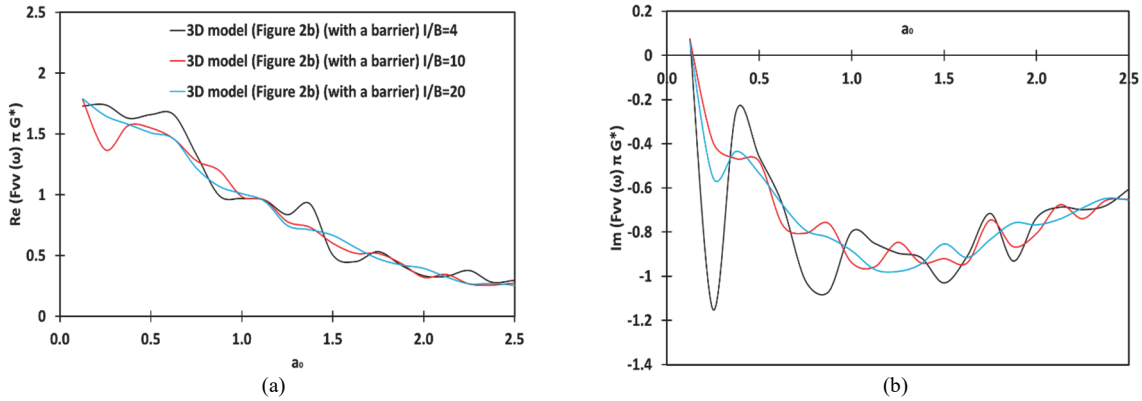

(a) (b)

Fig. 12 (a) Real and (b) imaginary compliance functions for the cases: with a concrete barrier for $I/B = 4$, 10, and 20 (model 2)

where n is the vibration mode number, $n = 1, 2, 3, \ldots$; $V_R = KV_S$ is the Rayleigh wave velocity of the soil; $0.874 \le K \le 0.955$ depends on Poisson's ratio, for practical purposes $K = 1$ (Woods 1968), H is the depth of the soil column.

Table 3 First four natural frequencies of the model

n	Theoretical-frequency f_n (Hz)	Dimensionless-frequency a_0	Simulated-frequency (Hz)	The difference $f_{\text{simulated}} - f_n$
1	1.8	0.125	1.78	–0.02
2	5.41	0.375	5.34	–0.07
3	9.02	0.625	8.90	–0.12
4	12.63	0.875	12.46	–0.17

One of the material-damping effects is to reduce the infinite values (peaks) of the compliance-coefficients at the characteristic (eigen) frequencies of the soil profile. In the present study, the peaks correspond to f_1 and f_2, so no resonance phenomena arises. The first and the second theoretical natural-frequencies of Model 2, by application of the above formula, are: $f_1 = 1.8$ Hz, $f_2 = 5.41$ Hz. The simulated ones, corresponding to the peaks of $a_0 = 0.125$ and $a_0 = 0.375$, are respectively equal to $f_1 = 1.78$ Hz, $f_2 = 5.34$ Hz. It can be noted that the theoretical and the simulated-natural frequency values f_1 and f_2 are very close. This explains the peaks appearing in the imaginary coefficient curves of the compliance (Fig. 8, for the case without a trench) for the aforementioned a_0 values. The peaks correspond to the first and the second natural-frequencies of the 3D FE Model 2 as shown in Fig. 2(b). Knowing the f_1 and f_2 values is indeed crucial in structural dynamics, as they represent the natural frequencies of the system. By reducing the vibrations at these frequencies, engineers can design structures to better withstand the stresses produced by vertical vibrations. The use of the reducing source-vibrations technique, as demonstrated in the present study, can help achieve this goal and improve the overall performance of structural foundations, particularly for machine-foundations. The accuracy of the model and the results obtained from the analysis confirm the usefulness of this technique in reducing vibrations and protecting structures against potential damage.

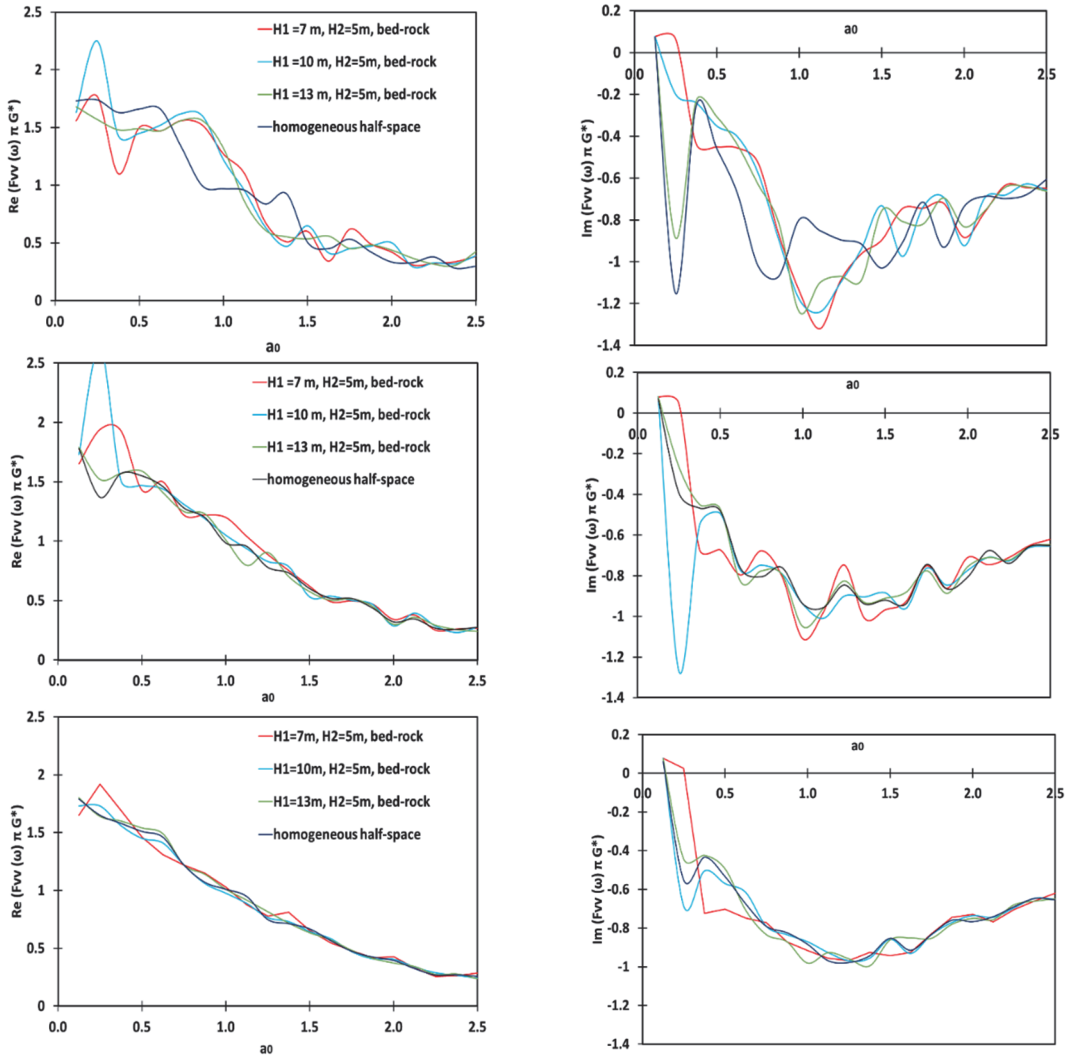

Fig. 13 (a) Real and (b) imaginary compliance functions of the cases from top to bottom: $I/B = 4$; $I/B = 10$; $I/B = 20$, the model of a homogeneous half-space with $H_1 = 13$ m, and the model of the soil layer limited by a rigid bed-rock with: ($H_1 = 13$ m, $H_2 = 5$ m), ($H_1 = 10$ m, $H_2 = 5$ m), ($H_1 = 7$ m, $H_2 = 5$ m).(Comparison between Model 2 and Model 3)

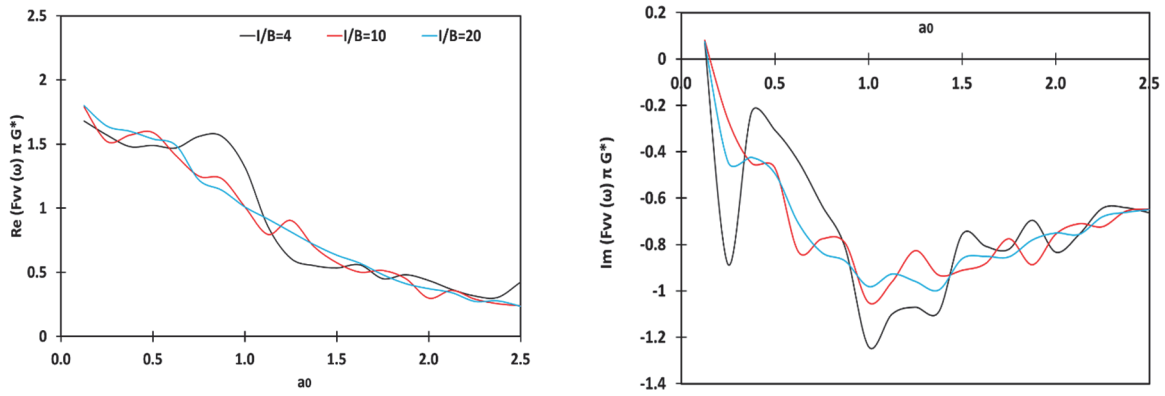

(a) (b)

Fig. 14 (a) Real and (b) imaginary compliance functions of the cases: I/B = 4, 10, 20, the model of the soil layer limited by a rigid bed-rock with: (H_1 = 13 m, H_2 = 5 m)

Figure 13 indicates that Model 3 located at a depth superior to 13B behaves in the same way as a homogeneous half-space model (black versus green curves).

Figure 14 shows that in presence of a bedrock, using an encircling concrete barrier at a distance of I/B = 4 is more effective in terms of vibration reduction level than using it at the distance of I/B = 10 or 20, particularly for $a_0 < 1$. The vibration waves that are reflected by the barrier and those reflected by the rigid bed-rock, propagate upward and then reflected at the free surface of the soil and at the footing surface.

Above the second natural-frequency, the compliance coefficients, particularly the imaginary ones, are almost frequency-independent. The difference between the theoretical and simulated frequency-values increases, considering the natural frequencies of the model that are above the second one is quite difficult, and this explains one of the weaknesses of using the FEM toward high frequencies, particularly, when the soil damping ratio is not equal to zero.

Now, civil engineers can have an overall index on how to design and install a concrete barrier in either a homogeneous half-space or a soil layer limited by a rigid bedrock models, using the findings plotted in Figs. 12 and 14 respectively. Defining the soil profile then defining the frequency a_0 values and finally selecting I/B suitable for sufficient vibration reduction level.

6. CONCLUSIONS

The study aims to analyze the impact of a vibration-reducing barrier around a footing in two different models: a homogeneous half-space model and a soil over a rigid bed-rock model. The study considers three different I/B ratios, namely I/B = 4, 10, and 20. The analysis focused on the compliance function coefficients of the models for vertical vibration, considering only V_{SV} and V_R waves. The aim is to investigate the effectiveness of the barrier in vibration reduction level and its effects on the compliance function coefficients of the models. The results suggest that the technique is more effective particularly for $a_0 \leq 1$. In a homogeneous half-space model, when the barrier installed farther from the footing, the model becomes less flexible due to the longer path that the vibration waves must travel towards the barrier and reflected back from it. The greater the distance between the footing and the barrier, the greater the geometric damping becomes. Additionally, Rayleigh waves dominate the model. In contrast, for one layer soil profile limited by a rigid bedrock, the model becomes less flexible when the barrier installed closer to the footing, and the body waves (in the present study, shear waves V_{SV}) dominate the model.

These findings suggest that a 3D FE model using the appropriate range of a_0 (from 0.1 to 2.5) can provide accurate predictions of the benefits of using vibration-barrier techniques against source-vibrations, as no significant changes in compliance coefficients values recorded for $a_0 > 1.5$, unlike the fluctuation and the instability of the results noticed for a 2D model. Moreover, choosing a finite element modeling with 30B of width and 15B of depth seems to be convenient to simulate the real behavior of a 3D model. The compliance coefficients curves plotted for a homogeneous half-space model with a vibration-reducing barrier installed at I/B = 20, can be also used for a one layer soil limited by a rigid bedrock model that is located at a depth of 13B or deeper.

Future research could build upon these findings by exploring the effects of the barrier in different soil types and conditions, as well as under different types of vibrations and loading conditions. This could help provide a more comprehensive understanding of the technique's effectiveness and inform its practical application in various engineering projects..

ACKNOWLEDGMENT

The authors would like to thank the Civil and Environmental Engineering Laboratory, LGCE University of Jijel, Algeria for their technical support. These supports made this study and further research possible.

FUNDING

The authors received no funding for this work.

CONFLICT OF INTEREST STATEMENT

The authors declare that there is no conflict of interest

DATA AVAILABILITY STATEMENT

The data and/or computer codes used/generated in this study can be downloaded at https://www.codeaster.org/spip.php?_rubrique7

NOTATIONS

$a_0 = \frac{\omega B}{V}$	dimensionless frequency
B	half side of the square foundation (m)
E	elasticity modulus (MPa)
$F_{ij}(\omega) = K_{ij}^{-1}(\omega)$	compliance functions matrix
f	maximum frequency of V (Hz)
f_n	theoretical natural-frequency of the model (Hz)
G^*	complex shear modulus
H_1	depth of the soil layer (m)
H_2	depth of the bedrock (m)
HTR	depth of the barrier (m)
I	distance between the mid-point of the footing and of the barrier (m)
$K_{ij}(\omega)$	impedance functions matrix
$k_{ij}(\omega)$, $c_{ij}(\omega)$	impedance coefficients
K_{stij}	static stiffness
Δl	size of the mesh element
S	distance between the mid-point of the barrier and the boundary of the model (m)
T	thickness of the barrier (m)
V	vertical unit steady state force (N)
v	complex correspondent displacement produced by V (m)
v/V	compliance function (m/N)
V_b, V_s	barrier and soil shear-wave velocities, respectively
V_R	velocity of Rayleigh waves
β	material damping ratio (hysteretic)
λ_{min}	shortest wavelength (m)
ν	Poisson's ratio
ρ	mass density (kg/m^3)
ρ_b, ρ_s	barrier and soil densities, respectively
ω	maximum pulsation of V ($\omega = 2\pi f$)

REFERENCES

Adam, M. and Estorff, O.V. (2005). "Reduction of train-induced building vibrations by using open and filled trenches." *Computers & Structures*, **83**(1), 11-24. https://doi.org/10.1016/j.compstruc.2004.08.010

Alzawi, A. and El-Naggar, M.H. (2011). "Full scale experimental study on vibration scattering using open and in-filled (GeoFoam) wave barriers." *Soil Dynamics and Earthquake Engineering*, **31**, 306-317. https://doi.org/10.1016/j.soildyn.2010.08.010

Amrane, A., Bourahla, N., Hassein-Bey, A., and Khelif, A. (2019). "Protection of structures subject to seismic and mechanical vibrations using periodical networks." *Journal of Materials and Engineering Structures*, **6**, 565-581.

Barkan, D.D. (1962). *Dynamics of Bases and Foundations*. New York, NY, USA: McGraw-Hill.

Bougressi, A., Bourahla, N., and Doufene M.A. (2017). "Potential of periodic networks for seismic isolation of sites." Tran-Nguyen HH., Wong H., Ragueneau F., Ha-Minh C., Eds., *Proceedings of the 4th Congrès International de Géotechnique - Ouvrages-Structures. CIGOS 2017*. Lecture Notes in Civil Engineering, **8**, Springer, Singapore.

Castellani, A. (1974). "Boundary conditions to simulate an infinite space." Istituto di Scienza a Tecnica delle Costruzioni, Politecnico di Milano.

Dobry, R. and Gazetas, G. (1986). "Dynamic response of arbitrarily shaped foundations." *Journal of Geotechnical Engineering*, **112**(2).

Dudchenko, A., Dias, D., and Kuznetsov, S.V. (2021). "Vertical wave barriers for vibration reduction." *Archive of Applied Mechanics*, **91**(1), 257-276. https://doi.org/10.1007/s00419-020-01768-2

Dudchenko, A., Dias, D., and Kuznetsov, S. (2022). "Pile rows for protection from surface waves," *Proceedings of FORM 2021*, 433-445.

Elsabee, F. (1975). *Static Stiffness Coefficients for Circular Foundations Embedded in an Elastic Medium*. M.S. Thesis, Department of Civil Engineering, M.I.T.

Fukuwa, N. and Nakai, S. (1989). "A study on lateral dashpots for soil-structure interaction and its application to a simplified technique." *Japanese Society of Soil Mechanics and Foundation Engineering*, **29**(3), 25-40.

Gazetas G. (1975). *Dynamic Stiffness Functions of Strip and Rectangular Footings on Layered Media*. M.S. Thesis, Department of Civil Engineering, M.I.T.

Gazetas, G. (1983). "Analysis of machine foundation vibrations: State of the art." *International Journal of Soil Dynamics and Earthquake Engineering*, **2**(1), 2-42.

Jazebi, M., Ahmadi, M.M., Saberian, M., Li, J., and Sahebalzamani, P. (2022). "Performance of open and in-filled (geofoam) trenches in mitigatingground-borne vibrations induced by impact loading." *International Journal of Pavement Research and Technology*, 1-13. https://doi.org/10.1007/s42947-022-00159-w

Jingbo, L., Yixin, D., Xiuli, D., Zhenyu, W., and Jun, W. (2006). "3D viscous-spring artificial boundary in time domain." *Code-Aster Manual (version 13.4). Earthquake Engineering and Engineering Vibration*, **5**(1).

Kausel, E. and Ushijima, R. (1979). *Vertical and Torsional Stiffness of Cylindrical Footings*. Research Report R79-6, MIT, Sponsored by the National Science Foundation Division of Adv. Environmental Research and Technology.

Klein, R., Antes, H., and Houedec, Le. D. (1997). "Efficient 3D modelling of vibration isolation by open trenches." *Computer and Structure*, **64**, 809-817.

Kuhlemeyer, R.L. and Lysmer, J. (1973). "Finite element accuracy for wave propagation problems (Technical note)." *Journal of the Soil Mechanics and Foundations Division*, ASCE, 99, SM5, 421-427. https://doi.org/10.1061/JSFEAQ.0001885

Lin, G., Han, Z., and Li, J. (2013). "An efficient approach for dynamic impedance of surface footing on layered half-space." *Soil Dynamics and Earthquake Engineering*, **49**, 39-51. https://doi.org/10.1016/j.soildyn.2013.01.008

Luco, J.E. (1974). "Impedance functions for a rigid foundation on layered medium." *Nuclear Engineering and Design*, **31**(2), 204-217.

McNeill, R., Margason, B.E., and Babcock, F.M. (1965). "The role of soil dynamics in the design of stable test pads." *Guidance Control Conference*, Woodward-Clyde-Sherard and Associates Consulting Soil and Foundation Engineers, Oakland, California, 366-375.

Messioud, S., Dias, D., and Sbartai, B. (2017). "Estimation of dynamic impedance of the soil-pile-slab and soil-pile-mattress-slab systems." *International Journal of Structural Stability and Dynamics*, **17**(6), 17. https://doi.org/10.1142/S0219455417500572

Messioud, S., Dias, D., and Sbartai, B. (2019). "Influence of the pile toe condition on the dynamic response of a group of pile foundations." *International Journal of Advanced Structural Engineering*, **11**, 55-66. https://doi.org/10.1007/s40091-019-0217-5

Messioud, S., Okyay, U.S., Sbartai, B., and Dias, D. (2016). "Dynamic response of pile reinforced soils and piled foundations." *Geotechnical and Geological Engineering*, **34**, 789-805. https://doi.org/10.1007/s10706-016-0003-0

Miller, G.F. and Pursey, H. (1955). "On the partition of energy between elastic waves in a semi-infinite solid." *Proceedings of the Royal Society of London*, *Series A, Mathematical and Physical Sciences*, **233**(1192), 55-69.

Mino, G.D., Giunta, M., and Liberto, C.M.D. (2009). "Assessing the open trenches in screening railway ground-bornevibrations by means of artificial neural network." Hindawi Publishing Corporation, *Advances in Acoustics and Vibration*, 2009, 942787. https://doi.org/10.1155/2009/942787

Neghmouche, Y., Messioud, S., and Dias, D. (2022). "Dynamic response of soil-piles-mattress-slab and soil-piles-slab systems under seismic loading." *Journal of GeoEngineering*, **17**(2), 89-101. https://doi.org/10.6310/jog.202206_17(2).3

Pecker, A. (1984). "Dynamique des sols." Presses de l'école nationale des ponts et chaussées.

Saikia, A. (2014). "Numerical study on screening of surface waves using a pair of softer backfilled trenches." *Soil Dynamics and Earthquake Engineering*, **65**, 206-213. https://doi.org/10.1016/j.soildyn.2014.05.012

Terzi, V. (2020). "Impedance functions of a strip foundation in presence of a trench." *European Journal of Environmental and Civil Engineering*, 1-38. https://doi.org/10.1080/19648189.2020.1805023

Wolf, J.P. (1989). "Soil-structure-interaction analysis in time domain." *Nuclear Engineering and Design*, **111**(3), 2, 381-393.

Wolf, J.P. and Deeks, A.J. (2004). *Foundation Vibration Analysis: A Strength-of-Materials Approach*. Elsevier, Linacre House, Jordan Hill, Burlington, MA.

Woods, R.D. (1968). *Screening of Surface Waves in Soil*. Ph.D. Dissertation, University of Michigan.